

# An ion-implanted silicon single-electron transistor

V.C. Chan,\* D.R. McCamey, T.M. Buehler,† A.J. Ferguson, D.J. Reilly,‡ A.S. Dzurak, and R.G. Clark

Centre for Quantum Computer Technology, Schools of Physics and Electrical Engineering  
& Telecommunications, The University of New South Wales, NSW 2052, Sydney Australia

C. Yang and D.N. Jamieson

Centre for Quantum Computer Technology, School of Physics, University of Melbourne, VIC 3010, Australia

(Dated: November 3, 2018)

We report on the fabrication and electrical characterization at millikelvin temperatures of a novel silicon single-electron transistor (Si-SET). The island and source-drain leads of the Si-SET are formed by the implantation of phosphorus ions to a density above the metal-insulator-transition, with the tunnel junctions created by undoped regions. Surface gates above each of the tunnel junctions independently control the tunnel coupling between the Si-SET island and leads. The device shows periodic Coulomb blockade with a charging energy  $e^2/2C_\Sigma \sim 250 \mu\text{eV}$ , and demonstrates a reproducible and controllable pathway to a silicon-based SET using CMOS processing techniques.

PACS numbers: 61.72.Tt, 73.23.Hk, 85.35.Gv

Single-electron transistors (SETs) have excellent potential as elementary devices in large scale circuits due to their small dimensions and low power dissipation. Applications for SETs in single-electron logic and memory cells<sup>1,2</sup> have also been demonstrated. Silicon-based SETs (Si-SETs) are of particular interest because of their compatibility with CMOS technology. While the fabrication of Si-SETs devices is a non-trivial process, a number of different approaches have been demonstrated such as gated two-dimensional electron gases (2DEGs)<sup>8</sup>, pattern dependent etching of silicon-on-insulator (SOI) material<sup>9,10</sup>, and random formation of Coulomb islands by nano-particles or defects in silicon<sup>3,4,5,6,7</sup>. Some difficulties of integrating such approaches into more complex single-electron circuits include inconsistent island formation resulting in random electron potentials and excessive gating requirements for electrostatically defining Coulomb islands and tunnel junctions.

The work presented in this letter features a Si-SET comprising of a single well-defined island and source-drain leads fabricated by a patterned phosphorus ion implantation process. This approach is *not* reliant on random island formation, and offers a new method for *controlled, reliable and reproducible* formation of Coulomb islands. This Si-SET essentially consists of two nano-scale metal-oxide-semiconductor field effect transistors (MOSFETs) in series with a micron scale central island, with the MOSFETs acting as tuneable tunnel junctions. As the island is solely defined by the patterned ion implantation, no gates are required to electrostatically define the island structure. Furthermore, the controlled formation of well-

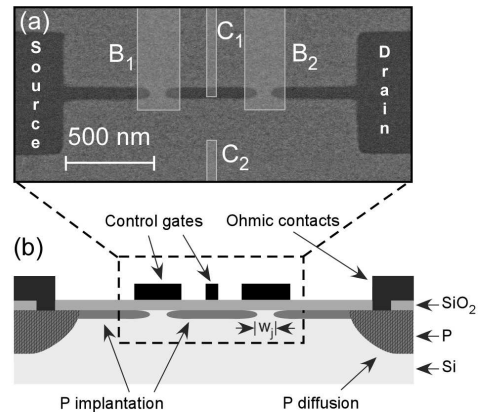


FIG. 1 (a) Scanning electron micrograph of a device prior to RTA. The darker areas indicate regions of phosphorus ion implantation damage. Surface gates are shown schematically. (b) Cross-section schematic of the device showing the phosphorus implanted area, phosphorus diffusion, ohmic contacts and surface gates.

defined islands makes the coupling of multiple single-electron devices for more complex circuits a simpler task. We discuss the device fabrication and electrical measurements performed at  $T = 50 \text{ mK}$  in which Coulomb blockade behavior is observed.

Devices were fabricated on a high resistivity ( $> 5 \text{ k}\Omega\text{cm}$ ) n-type silicon wafer. Firstly, ohmic contacts for the source and drain leads of the device were defined via phosphorus diffusion. A 5 nm gate oxide was then grown using a thermal oxidation process. Electrical characterization of (large-scale) MOSFET devices fabricated with gate oxides grown using the same process indicate typical trap densities of  $2 \times 10^{11} \text{ cm}^{-2}$  at  $T = 4.2 \text{ K}$ <sup>11</sup>. High-resolution TiPt (15 nm Ti, 65 nm Pt) alignment markers, 100 nm  $\times$  100 nm in dimension, were de-

\*Electronic address: victor.chan@bigpond.com

†Now at ABB Switzerland, Corporate Research.

‡Now at Dept. Physics, Harvard University, Cambridge, 02138, USA.

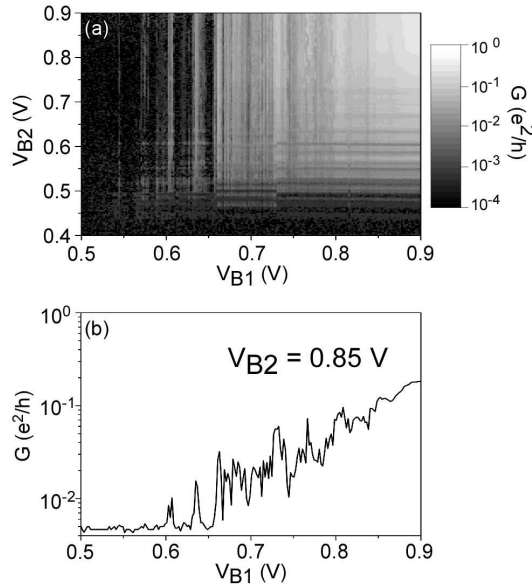


FIG. 2 (a) Si-SET ( $w_j = 150$  nm) conductance intensity plot as a function of  $V_{B1}$  and  $V_{B2}$ . Resonances, most likely due to defects in the tunnel junctions, are observed in the vertical and horizontal axis indicating independent control of the tunnel barriers. (b) Single trace taken from (a) at  $V_{B2} = 0.85$  V showing increasing conductance with positive voltage applied to  $B_1$ .  $V_{ac} = 100$   $\mu$ V.  $T = 50$  mK.

fined by electron-beam lithography. These markers were used to align subsequent e-beam lithography steps with an accuracy of  $\leq 50$  nm, whilst being able to withstand subsequent thermal processes. A 150 nm thick poly-methyl-methacrylate (PMMA) resist was applied and patterned by e-beam lithography for use as a mask for ion implantation. The dimensions of the SET island were designed to be 70 nm  $\times$  500 nm. A number of different devices were fabricated with intrinsic tunnel junction widths  $w_j$  of 100 nm and 150 nm (see figure 1(b)).

Phosphorus ions at 14 keV were implanted with an areal dose of approximately  $1.22 \times 10^{14}$  cm $^{-2}$  and a mean implantation depth of  $\sim 20$  nm. This equates to approximately 43000 ions in the island and a doping density of  $\sim 10^{19}$  cm $^{-3}$ . A scanning electron micrograph (SEM) of a device after ion implantation and removal of the PMMA mask is shown in figure 1, note the high contrast between the ion implanted and masked regions due to damage in the silicon crystal caused by the ion implantation. A rapid thermal anneal (RTA) at 1000°C for 5 sec was performed to repair implantation damage and electrically activate the phosphorus donors. Post-RTA SEM imaging of the implanted regions show significantly less contrast to the masked regions, indicating repair of the implantation damage. In the final step, four electrostatic control gates (shown schematically in figure 1) were fabricated by e-beam lithography using 60 nm PMMA resist and TiAu (10 nm Ti, 20 nm Au) metallization. Two barrier gates ( $B_1$  and  $B_2$ ) were defined over the tunnel junctions, one gate ( $C_1$ ) over the island, and the fourth gate ( $C_2$ ) a small distance away from the island.

Electrical measurements were carried out at  $T = 50$  mK in a

dilution refrigerator using standard lock-in techniques at frequencies  $< 200$  Hz. Initial characterization of these devices focussed on the effect of the electrostatic barrier gates on the tunnel junctions. Figure 2(a) shows the conductance of a device with 150 nm wide tunnel junctions as a function of  $V_{B1}$  and  $V_{B2}$ . The behavior observed in this device is representative of all of the devices that were measured. With increasing barrier gate voltage, the device conductance is increased as expected for an enhancement-mode MOSFET (see figure 2(b)). Resonances observed in the device conductance are visible in figure 2(a) as vertical and horizontal lines, and indicate that each barrier gate is primarily coupled to its respective tunnel junction. These resonances most likely arise from the random potentials in the tunnel junctions, due to stray dopants, charge traps and other defects. These form unintentional islands that exhibit either Coulomb blockade or resonant tunnelling phenomena.<sup>12</sup> Even with these resonances present, the measurements indicate good gate control of the overall conductance of the tunnel junctions.

In figure 3(a), the grey trace shows the conductance of a Si-SET with 100 nm wide tunnel junctions as a function of  $V_{C1}$  with  $V_{B1} = V_{B2} = 0$  mV and  $V_{SD} = 350$   $\mu$ V. In the measurement, periodic Coulomb blockade oscillations are observed indicating a constant capacitance between the gate and the Si-SET island. The consistent form of the conductance peaks also indicates that the tunnel junctions are not significantly changing. Figure 3(b) shows a bias spectroscopy measurement for the same device. Coulomb charging diamonds with a constant charging energy are observed, consistent with charging a single metallic island as opposed to a random minimum potential in the tunnel junctions. This is in contrast to Coulomb blockade associated with unintentionally formed islands in the channel of FETs where the charging energy and periodicity changes significantly with island occupancy. In common with other SETs, the device is sensitive to 1/f charge noise and nearby two-level fluctuators (TLF) which perturb the device conductance, as observed in figure 3 (b) around  $V_{C2} = 110$   $\mu$ V.

Further measurements were performed on the Si-SET with 100 nm wide tunnel junctions to observe how gate tuning of the tunnel barriers could be used to control the device conductance whilst maintaining Coulomb blockade behavior. A number of different voltages were applied to the barrier gates ( $B_1$  and  $B_2$ ). Under low source-drain bias conditions and  $V_{B1} = V_{B2} = 0$  V, the device conductance is actually below the measurable threshold for standard lock-in amplifier techniques ( $I_{SD} < 1$  pA). At  $V_{B1} = V_{B2} = -200$  mV, the barrier gates are biased close to some resonance in the barriers which results in an overall increase in the conductance of the device. The black trace in figure 3(a) shows the Si-SET conductance under these barrier conditions and Coulomb blockade oscillations are clearly observed. In comparison to the grey trace in the same figure, which shows Si-SET conductance when  $V_{B1} = V_{B2} = 0$  mV and  $V_{SD} = 350$   $\mu$ V, the peak conductance observed in the black trace is an order of magnitude higher ( $G_{SET}$  (grey)  $\sim 7 \times 10^{-3}$  e $^2$ /h and  $G_{SET}$  (black)  $\sim 4 \times 10^{-2}$  e $^2$ /h). The periodicity of the oscillations are consistent between both traces reinforcing the notion that

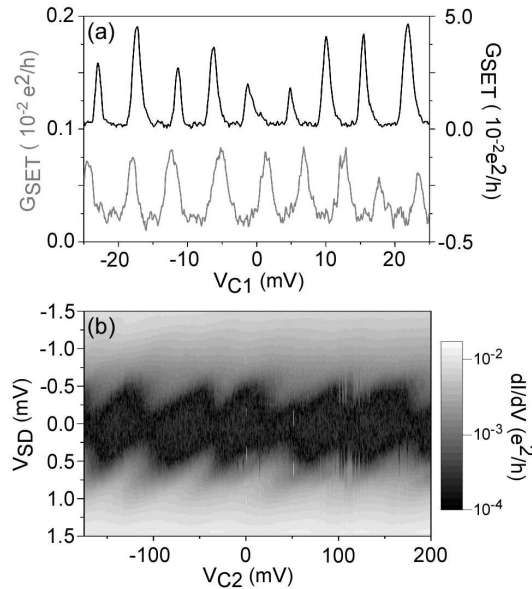


FIG. 3 (a) Si-SET ( $w_j = 100$  nm) source-drain conductance as a function of  $V_{C1}$  shows Coulomb blockade oscillations for  $V_{B1} = V_{B2} = 0$  mV (grey trace,  $V_{SD} = 350\mu\text{V}$ ) and  $V_{B1} = V_{B2} = -200$  mV (black trace,  $V_{SD} = 0\mu\text{V}$ ).  $V_{ac} = 50\mu\text{V}$ .  $T = 50$  mK. (b) Si-SET ( $w_j = 100$  nm) bias spectroscopy measurement. Coulomb blockade diamonds are observed indicating a device charging energy  $e^2/2C_\Sigma$  of  $\sim 250$   $\mu\text{eV}$ . Around  $V_{C2} = 110$   $\mu\text{V}$  the device conductance is perturbed by charge noise fluctuation.  $V_{ac} = 50\mu\text{V}$ .  $T = 50$  mK.

Coulomb blockade in a single well-defined metallic island is being observed. Similar behavior is seen for barrier conditions where large positive voltages are applied to the barrier gates to increase the transparency of the tunnel junctions.

From the bias spectroscopy data shown in figure 3(b), the charging energy of the island in the Si-SET with 100 nm wide tunnel junctions is determined to be  $e^2/2C_\Sigma \sim 250$   $\mu\text{eV}$  with a total capacitance  $C_\Sigma$  of 320 aF. The capacitances of gates  $C_1$  and  $C_2$  to the island are determined from the period of the measured Coulomb blockade oscillations to be 27 aF and 2.1 aF respectively. The capacitances of barrier gates  $B_1$  and  $B_2$  to the island were not measured for this device, however these values have been measured for other devices and are typically of order 100 aF. The asymmetry of the Coulomb diamonds is a result of the different capacitances between the implanted island and the source and drain leads, which are determined from the Coulomb diamonds to be 21 aF and 55 aF. This difference in capacitance can be attributed to the barriers being of slightly different dimensions and differences in their complex potential landscape.

A proof-of-principle has been demonstrated for the controlled formation of Coulomb blockade islands using CMOS processing techniques. The Si-SET demonstrates highly controllable single-island charging behavior due to the well-defined electron potential. The tunnel coupling between the

Coulomb blockade island and leads can be changed by using electrostatic gates above the tunnel junctions (MOSFETs). The development of Si-SET as elements in more complex single-electron circuits requires the ability to controllably couple multiple islands and future work will focus on this. Whilst characterization of this device demonstrates Si-SET behavior at low temperature ( $T = 50$  mK), further development of this fabrication technique will involve scaling down of the island size to enable the charging energy  $E_C$  to dominate at higher temperatures ( $E_C > k_B T$ ). In addition, related devices may provide a platform for the study of electron transport between locally doped regions in silicon, which is of particular relevance to silicon-based quantum computing<sup>13,14,15</sup>.

The authors would like to thank S.E. Andresen, J.C. McCallum, M. Lay, C.I. Pakes, and S. Prawer for helpful discussions and E. Gauja, R. P. Starrett, D. Barber, G. Tamanyan and R. Szymanski for their technical support. This work was supported by the Australian Research Council, the Australian Government and by the US National Security Agency (NSA), Advanced Research and Development Activity (ARDA) and the Army Research Office (ARO) under contract number DAAD19-01-1-0653.

## References

- [1] C. P. Heij, P. Hadley, and J. E. Mooij, *Appl. Phys. Lett.* **78**, 1140 (2001).
- [2] N. J. Stone and H. Ahmed, *Appl. Phys. Lett.* **73**, 2134 (1998).
- [3] T. Baron, P. Gentile, N. Magnea, and P. Mur, *Appl. Phys. Lett.* **79**, 1175 (2001).
- [4] F. Boeuf, X. Jehl, M. Sanquer, and T. Skotnicki, *IEEE Trans. Nanotech.* **2**, 144 (1997).
- [5] M. Sanquer, M. Specht, L. Ghenim, S. Deleonibus, and G. Guegan, *Phys. Rev. B* **61**, 7249 (2000).
- [6] A. Nakajima, T. Futatsugi, H. Nakao, T. Usuki, N. Horiguchi, and N. Yokoyama, *J. Appl. Phys.* **84**, 1316 (1998).
- [7] H. Kondo, H. Iwano, O. Nakatsuka, K. Kaga, S. Zaima, and Y. Yasuda, *Jpn. J. Appl. Phys.* **36**, 4046 (1997).
- [8] M. Khouri, A. Gunther, D. P. Pivin, M. J. Rack, and D. K. Ferry, *Jpn. J. Appl. Phys.* **38**, 469 (1999).
- [9] K. Nishiguchi, H. Inokawa, Y. Ono, A. Fujiwara, and Y. Takahashi, *Appl. Phys. Lett.* **85**, 1277 (2004).
- [10] E. G. Emiroglu, D. G. Hasko, and D. A. Williams, *Appl. Phys. Lett.* **83**, 3942 (2003).
- [11] D. R. McCamey, M. Francis, J. C. McCallum, A. R. Hamilton, A. D. Greentree, and R. G. Clark, *Semicond. Sci. Technol.* **20**, 363 (2005).
- [12] M. Sanquer, M. Specht, L. Ghenim, S. Deleonibus, and G. Guegan, *Ann. Phys. (Leipzig)* **8**, 743 (1999).
- [13] L. C. L. Hollenberg, A. S. Dzurak, C. Wellard, A. R. Hamilton, D. J. Reilly, G. J. Milburn, and R. G. Clark, *Phys. Rev. B* **69**, 113301 (2004).
- [14] T. Schenkel, A. Persaud, S. J. Park, J. Nilsson, J. Bokor, J. A. Liddle, R. Keller, D. H. Schneider, D. W. Cheng, and D. E. Humphries, *J. Appl. Phys.* **94**, 7017 (2003).
- [15] B. E. Kane, *Nature* **393**, 133 (1998).